

Chemodivergent Coupling of 1,3-Enynes with Anilines to Access Dihydropyrrole Skeleton under Palladium Catalysis

Received: 12 November 2025

Accepted: 19 February 2026

Published online: 03 March 2026

Check for updates

Su-Yang Xu^{1,2}, Xue-Ting Li^{1,2}, Zhi-Hui Wang^{1,2}, Ding-Wei Ji¹✉ & Qing-An Chen^{1,2}✉

2,5-Dihydropyrroles are prevalent structural motifs in various natural products and biologically active molecules. Conventional methods for constructing these heterocycles often rely on elaborate multi-step procedures or complex starting materials. Herein, we describe a palladium-catalyzed chemodivergent protocol for synthesizing functionalized 2,5-dihydropyrrole scaffolds from readily accessible 1,3-enynes and anilines. By modulating the relative rates of the selectivity-determining steps, either two-component annulation or three-component telomerization can be selectively achieved, affording two distinct types of functionalized 2,5-dihydropyrroles in excellent yields and with high selectivities. Mechanistic studies reveal that the reaction initially proceeds through 1,4-hydroamination of 1,3-enynes to generate an aminomethyl allene intermediate, followed by an intramolecular annulation affording 2-substituted 2,5-dihydropyrroles. This process is significantly accelerated in the presence of Pd(II) catalysts. However, employing Pd(0) precursors, strong acids, and excess ligand effectively decelerates this pathway, diverting the selectivity towards reaction with a second equivalent of 1,3-enyne to yield the telomeric products. This study not only provides an atom-economical method for constructing the 2,5-dihydropyrrole core but also offers a valuable strategy for the development of telomerization chemistry.

Efficient manipulation of reaction selectivity remains a permanent pursuit among the organic community. Fundamentally, the successful selectivity regulation depends on the ability to identify selectivity-determining intermediates and precisely modulate the relative rates of competing elementary steps. For instance, in a traditional two-component reaction, substrate **A** could react with substrate **B** to form the product **C** through the intermediate **I**, or the product **D** via the intermediate **II** (Fig. 1a). Product **C** predominates if the combined rate constants k_1 and k_3 significantly exceed k_2 and k_4 , whereas product **D** prevails under the opposite scenario^{1–9}. However, controlling selectivity becomes substantially more complex in reactions involving multiple equivalents of a substrate, such as telomerization (e.g.,

A + 2**B**), where additional key intermediates necessitate sophisticated reactivity regulation.

Nitrogen-containing heterocycles (*N*-heterocycles) are ubiquitous structural motifs found in numerous biologically active molecules and natural products. 82% of FDA-approved small-molecule drugs between 2013 and 2023 contain at least one *N*-heterocycle^{10,11}. However, while saturated and aromatic *N*-heterocycles are extensively studied, the synthesis and application of their semi-saturated counterparts remain significantly underdeveloped^{12–14}. Notably, 2,5-dihydropyrroles represent an important class of five-membered semi-saturated *N*-heterocycles with diverse pharmacological and biological activities (Fig. 1b)^{15–17}. Despite the potential, catalytic methods for the efficient

¹Dalian Institute of Chemical Physics, Chinese Academy of Sciences, 457 Zhongshan Road, Dalian, China. ²University of Chinese Academy of Sciences, Beijing, China. ✉e-mail: dingweiji@dicp.ac.cn; qachen@dicp.ac.cn

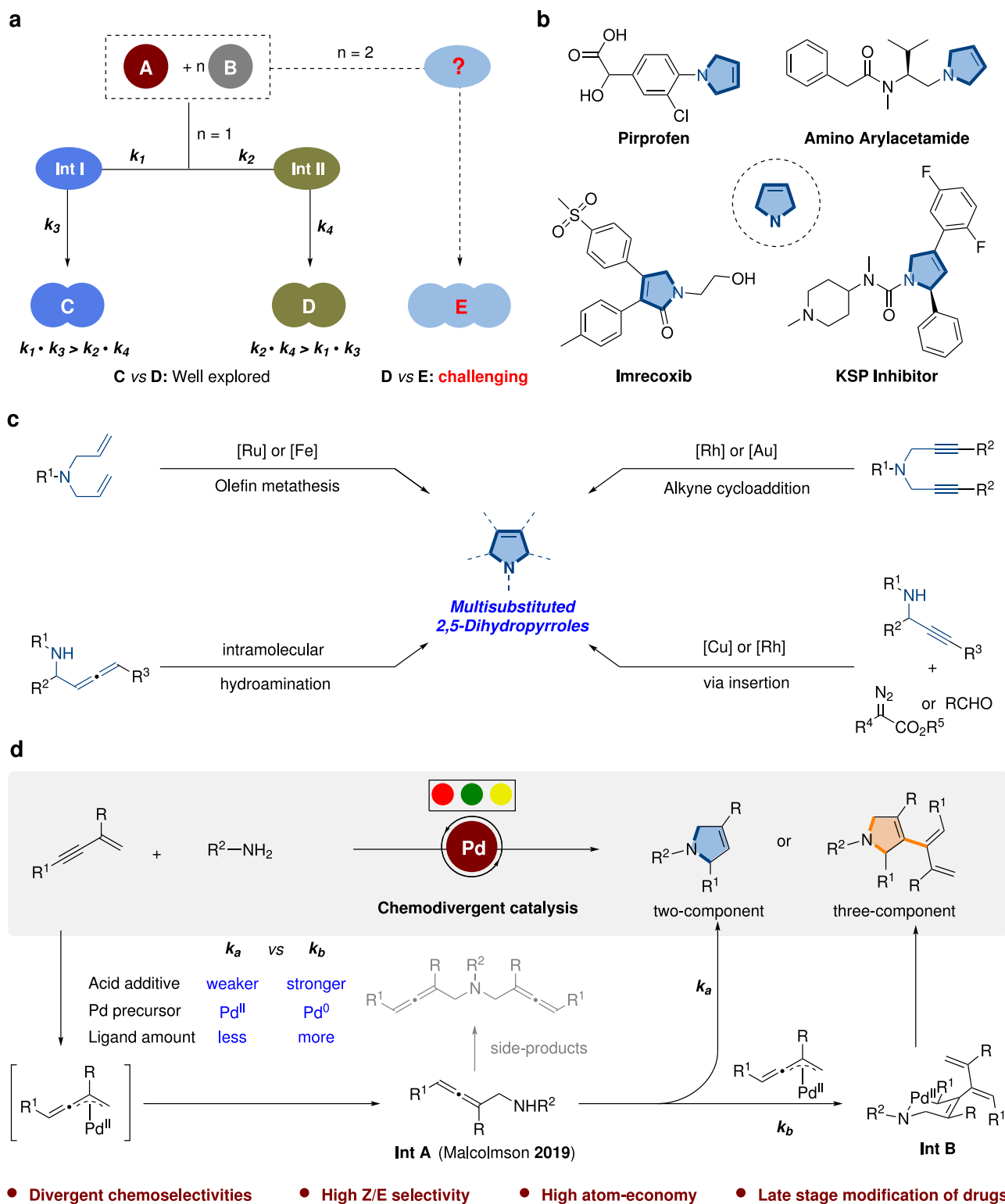


Fig. 1 | Transition-metal catalyzed synthesis of 2,5-dihydropyrroles. **a** The control of selectivity in organic reactions. **b** Bioactive molecules containing 2,5-dihydropyrrole motifs. **c** Representative strategies for building multi-substituted 2,5-

dihydropyrroles. **d** This work: Chemodivergent synthesis of 2,5-dihydropyrroles through the precise control over reaction rate.

construction of functionalized 2,5-dihydropyrroles lag far behind those for their saturated (pyrrolidines) or aromatic (pyrroles) analogs¹⁸. Existing approaches include olefin metathesis of *N,N*-diallylamine^{19–22}, Rh- or Au-catalyzed alkyne cycloadditions^{23–25}, and intramolecular hydroamination of allylamines or propargylamines^{26–28} (Fig. 1c). Huang, Reddy, and co-workers also reported an annulation

with diazo ester and propargyl amines via metal carbene intermediates^{29,30}. More recently, Zhou and co-workers developed a two-step synthesis involving propargylic amination³¹ (Fig. 1c). Although important, these methods often suffer from drawbacks such as multi-step sequences or the requirement of specialized starting materials. Consequently, the development of an atom- and step-

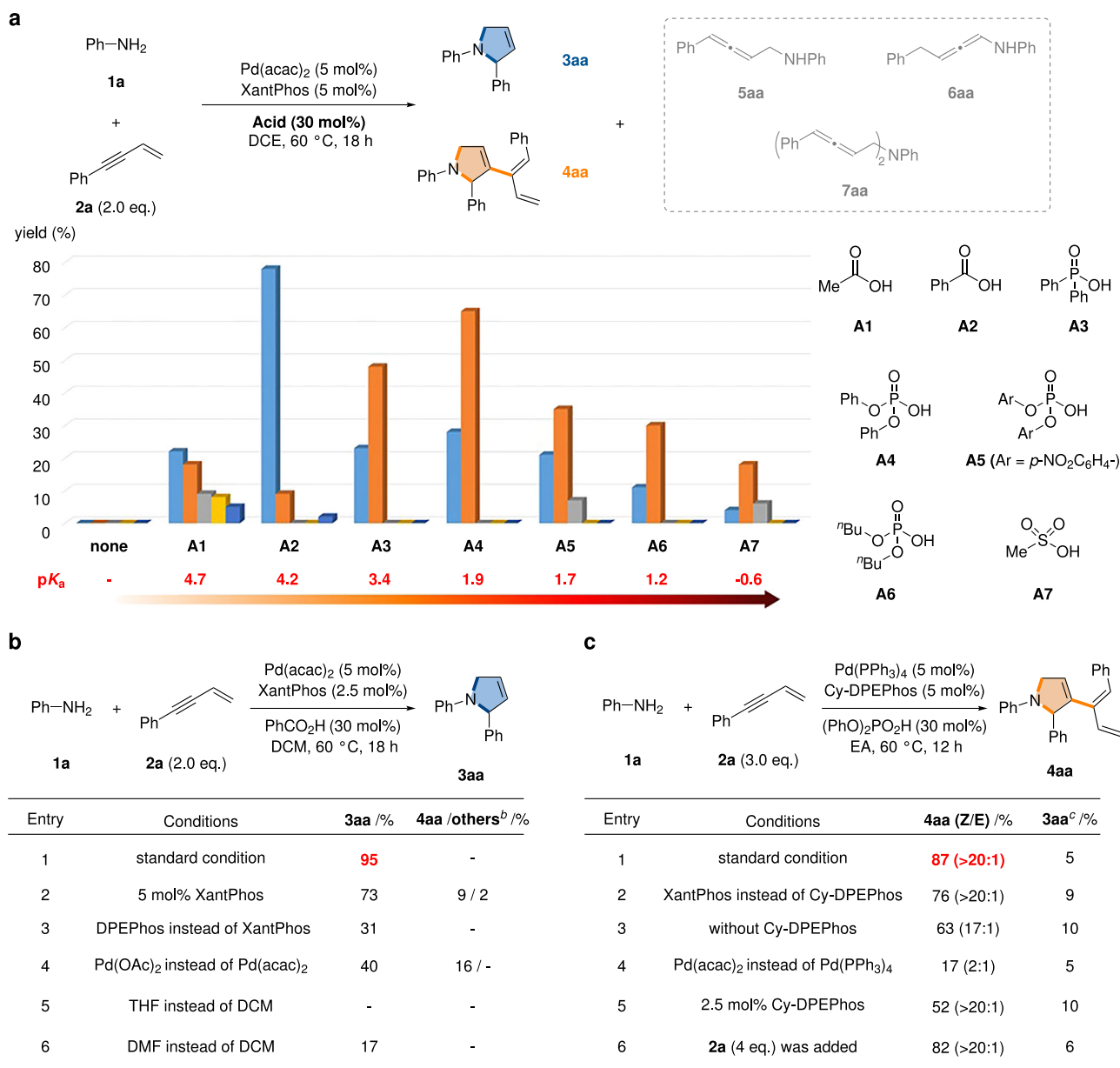


Fig. 2 | Optimization studies for chemodivergent coupling of 1,3-enyne with aniline. a Acid effects on Pd-Catalyzed cyclization reactions. **b** Evaluation of condition of product **3aa**. **c** Evaluation of condition of product **4aa**. ^aYields were

determined by ¹H-NMR analysis with CH₂Br₂ as internal standard. ^bTotal yields of other side-products **5aa-7aa**. ^cOther side-products **5aa-7aa** were not detected.

economical route to functionalized 2,5-dihydropyrroles from readily available substrates is still highly desirable.

Retrosynthetically, the successive hydroamination of 1,3-enynes with anilines provides a direct, atom-economical pathway to 2,5-dihydropyrrole scaffolds. However, the inherent versatile reactivity and high unsaturation of 1,3-enynes pose significant challenges for chemoselectivity control³²⁻⁴⁹. Building on our group's ongoing interest in divergent synthesis⁵⁰⁻⁵⁴, we envisioned an unprecedented chemodivergent approach to access functionalized 2,5-dihydropyrroles from 1,3-enynes and anilines. Notably, Malcolmson and co-workers have reported 1:1 coupling of 1,3-enynes with anilines in 2019, delivering amino allenes with an efficiency⁵⁵.

Herein we report a systematic modulation of the selectivity-determining step through synergistically tuning of ligands, acids and palladium precursors to realize the chemodivergent strategy and suppress other competing pathways, such as the formation of acyclic diamination byproducts (Fig. 1d). Our design centers on an initial Pd-

catalyzed hydroamination of 1,3-enyne with aniline, generating an allene intermediate **A**. This key intermediate **A** could then undergo either intramolecular hydroamination to afford the two-component dihydropyrrole product, or couple with a second molecule of 1,3-enyne to form **Int B** – a route to the telomeric dihydropyrrole product.

Results

Reaction optimization

We commenced this chemodivergent and atom-economic protocol using aniline **1a** and 1,3-enyne **2a** as model substrates (Fig. 2a). Given the crucial role of acid additives for in situ generation of metal-hydride species^{36,56-59}, we first carefully investigated a series of acids with varying pK_a values using Pd(acac)₂ and XantPhos as the catalytic precursor (Fig. 2a). While no reaction occurred in the absence of acid, employing 30 mol% acetic acid afforded dihydropyrrole **3aa** and telomerization product **4aa** in 22% and 18% yields, respectively, along with side-products **5aa-7aa** (combined 22% yield).

Encouragingly, replacing acetic acid with benzoic acid significantly improved the reaction, providing **3aa** in 78% yield with enhanced selectivity. To our surprise, stronger acids (**A3–A6**, $pK_a < 3.4$) effectively shifted the chemoselectivity towards the telomerization product **4aa**. Among them, diphenyl phosphate (**A4**) afforded **4aa** in the highest yield and selectivity. However, the reactivity was dramatically diminished when the very strong acid (MsOH, **A7**) was used. Consequently, benzoic acid (**A2**) and diphenyl phosphate (**A4**) were chosen as optimal additives.

With the acid additive identified, we then evaluated other reaction parameters for dihydropyrrole product **3aa** and telomerization product **4aa** separately (Fig. 2b, c and Supplementary Tables 1–9). In the presence of 30 mol% PhCO₂H, the desired product **3aa** was obtained in 95% yield with excellent selectivity using 5 mol% Pd(acac)₂ and 2.5 mol% XantPhos in DCM at 60 °C (Fig. 2b, entry 1). It should be noted that the loading amount of ligand significantly affected the reaction outcomes. When the amount of XantPhos was increased to 5 mol%, the yield of **3aa** decreased to 73%, accompanied by formation of **4aa** in 9% yield (entry 2). Screening other mono- and bidentate phosphine ligands confirmed XantPhos as optimal (entry 3 and Supplementary Table 4). Other palladium catalyst precursors, such as Pd(OAc)₂, resulted in reduced reactivities (entry 4 and Supplementary Table 3). Solvents THF and DMF proved unsuitable for the formation product **3aa** compared to DCM (entries 5–6).

Subsequently, we shifted our attention to the condition optimization for aminated telomerization reaction (Fig. 2c). To our delight, model product **4aa** was obtained in 87% yield with >20:1 Z/E selectivity upon switching to diphenyl phosphate as the acid additive in the presence of Pd(PPh₃)₄ and Cy-DPEPhos (entry 1, Supplementary Tables 7 and 8). Compared with Cy-DPEPhos, XantPhos exhibited lower activity and chemoselectivity for this transformation (entry 2 and Supplementary Table 8). This protocol could also proceed without additional ligand but in a decreased yield and selectivity (entry 3). When reactions were explored with other Pd^{II} or Pd⁰ catalyst precursors, the yields, as well as chemo- and stereoselectivities, decreased dramatically (entry 4 and Supplementary Table 7). Differing from product **3aa**, only 52% yield of **4aa** could be obtained when reducing the amount of ligand from 5 mol% to 2.5 mol% (entry 5). Further increasing the dosage of 1,3-enyne did not improve the yield of **4aa** (entry 6).

Substrate scope

With the optimized reaction conditions established, we then explored the substrate scope of this Pd-catalyzed sequential hydroamination of 1,3-enynes (Fig. 3a). With the aid of PhCO₂H, the model reaction between aniline **1a** and 1,3-enyne **2a** afforded **3aa** in 91% isolated yield. The structure of **3aa** was confirmed by single-crystal X-ray crystallography (CCDC: 2468082). Overall, this protocol exhibits good functional group tolerance, delivering the desired 2,5-dihydropyrroles in 38–93% yields (**3ab–3ra**). For example, anilines with electron-donating groups at either the *para*- or *meta*-position of the phenyl ring were all compatible under the standard conditions (**3ab–3ag**). It is worth noting that substituents at the *ortho*-position were also tolerated, affording products **3ah** and **3ai** in 46% and 89% yields, respectively. Anilines bearing electron-withdrawing groups were amenable to this transformation as well, constructing 2,5-dihydropyrroles **3aj–3an** in 56–92% yields. To our delight, the bromo group, which is sensitive and easily eliminated under palladium catalysis, remained intact under the current reaction conditions (**3am**). In addition, arylamines bearing naphthyl or heteroaromatic rings reacted smoothly with 1,3-enynes, producing the corresponding products in satisfactory yields (**3ao–3ar**). In contrast to arylamines, alkyl-substituted primary amines showed sluggishness under current protocol (for details, see unsuccessful substrates in Supplementary Information, Supplementary Fig. 1).

Next, 1,3-enynes bearing various substituents were investigated (Fig. 3b). 1,3-Enynes with substituents at the *para*-position on the phenyl ring, irrespective of their electron-donating or electron-withdrawing properties, all proceeded efficiently in this atom-economic transformation, affording the corresponding products in good to excellent yields (**3ba–3ka**). The sterically hindered substrate possessing a substituent at the *ortho*-position of the phenyl ring showed no significant decrease in reactivity (**3la**). When the phenyl ring was replaced with a naphthyl group or heterocyclic groups such as 3-pyridyl and 3-thienyl, the 1,3-enynes also proved viable, yielding the corresponding products in 50–91% yields (**3ma–3oa**). Besides aryl groups, alkyl-substituted 1,3-enynes also underwent the 1,4-cyclization smoothly, affording the desired products in moderate to good yields (**3pa–3qa**). In addition, 1,3-disubstituted 1,3-enyne was also an applicable substrate, furnishing a highly functionalized 2,5-dihydropyrrole (**3ra**) in 77% yield. Notably, all evaluated substrates exhibited excellent chemoselectivities. To access the asymmetric dihydropyrrole skeleton, condition optimizations of enantioselective hydroamination were carried out (for details, see Supplementary Information, Supplementary Table 10). Employing (*R*)-MeO-Biphep as chiral ligand and 3,5-di-*tert*-butylbenzoic acid as additive, product **3aa** could be obtained in 65% yield and 82% ee. The absolute configuration of chiral dihydropyrrole **3aa** was determined by single-crystal X-ray diffraction (CCDC: 2519020).

Subsequently, the generality of the Pd-catalyzed telomerization between 1,3-enynes and anilines was evaluated (Fig. 4). Under the standard conditions with diphenyl phosphate as the additive, model product **4aa** was isolated in 85% yield with exclusive stereoselectivity (>20:1 Z/E ratio, Fig. 4a). The stereo configuration of the product **4aa** was determined by ¹H-¹H NOESY spectra (see Supplementary Information for details). The reactions also proceeded smoothly with anilines bearing alkyl groups at the *para*- or *meta*-positions of the benzene ring (**4ab–4ad**). Despite its potential lability, versatile bromo group was tolerated to afford the target products in good yields, facilitating further derivatizations (**4ak** and **4al**). Substrates bearing stronger electron-withdrawing groups like trifluoromethyl and ester groups showed decreased reactivities under the standard conditions, requiring higher reaction temperatures (**4am–4an** vs. **4ao**). Polycyclic and heteroaryl amines were also feasible substrates, affording the products in decent yields (**4ap–4ar**). However, the telomerization reaction was sensitive to the steric hindrance of amines. The *ortho*-substituted arylamines were not applicable under current conditions (for details, see unsuccessful substrates in Supplementary Information, Supplementary Fig. 1).

This unprecedented telomerization also demonstrated good generality for 1,3-enyne substrates (Fig. 4b). A variety of 1,3-enynes bearing alkyl groups at the *para*-position reacted with aniline **1a** in high yields and with high Z/E selectivities (**4ba–4da**). A methyl group at the *ortho*-position of the phenyl ring was also compatible (**4ea**). Other electron-donating groups, such as methoxy (**4ia**), and amino (**4ja**), as well as electron-withdrawing groups like halogens (**4fa–4ha**), cyano, trifluoromethyl, ester, and phenyl (**4ka–4na**), all showed good compatibility under the current conditions. It is worth noting that the structure of **4ja** was further confirmed by single-crystal X-ray crystallography (CCDC: 2468080). 2-Naphthyl-substituted 1,3-enyne afforded product **4oa** in 85% yield with >20:1 Z/E selectivity. Heterocyclic substituents containing coordinating atoms, such as N and S, exhibited little influence on the reaction outcomes, as demonstrated by **4pa** and **4qa**. However, the reaction with alkyl-substituted 1,3-enyne resulted in an apparent decrease in stereoselectivity (**4ra**, 4:1 Z/E).

Mechanistic investigations

To elucidate the mechanism underlying this chemodivergent transformation, we conducted a series of mechanistic experiments. First, allene **5aa** was successfully isolated and subjected to the standard

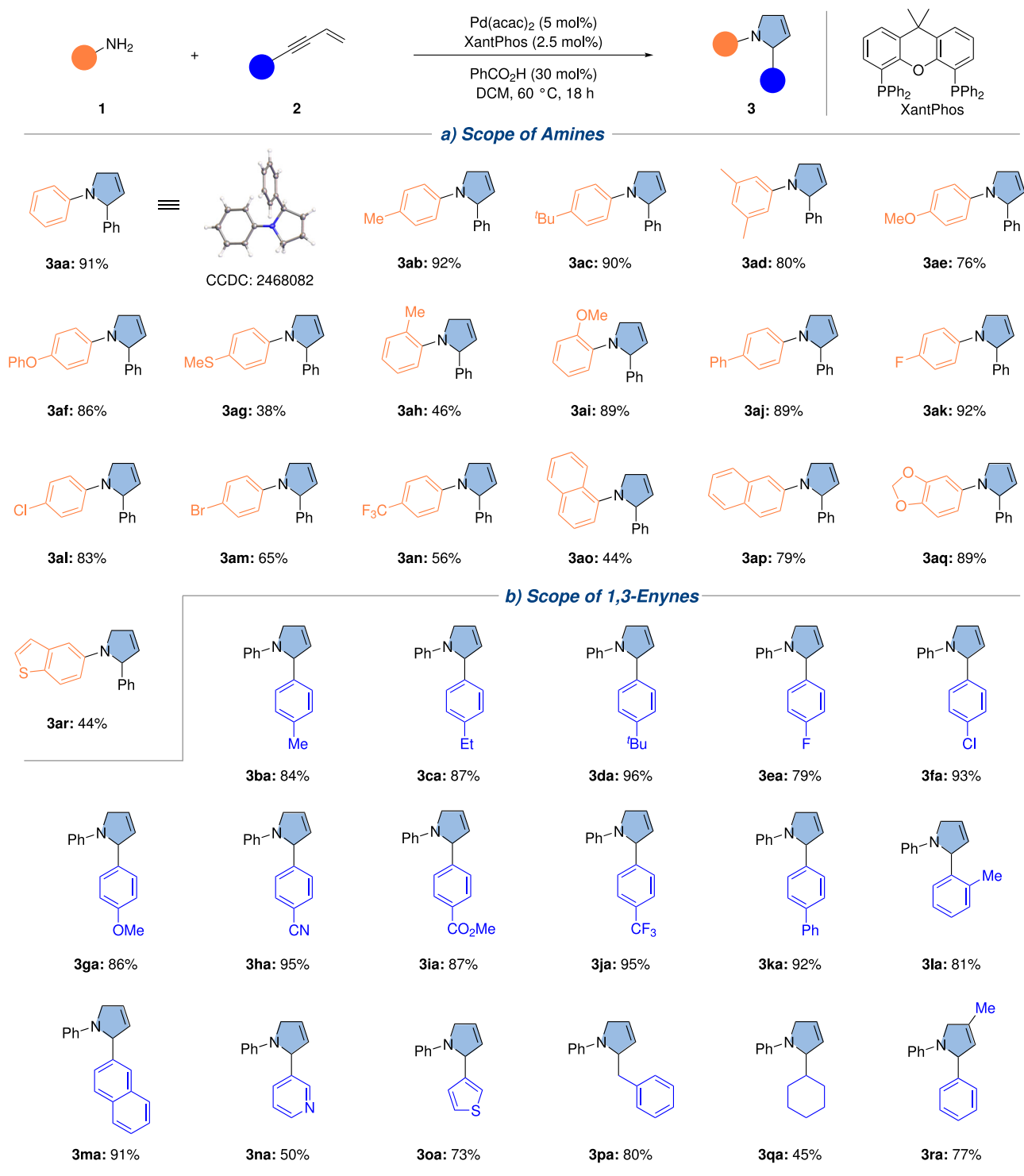


Fig. 3 | Substrate scope for Pd-catalyzed sequential hydroamination of 1,3-enynes. a Scope of Amines. **b** Scope of 1,3-Enynes. Condition: **1** (0.20 mmol), **2** (2.0 eq.), Pd(acac)₂ (5 mol%), XantPhos (2.5 mol%), PhCO₂H (30 mol%), DCM (1.0 mL), 60 °C, 18 h. Isolated yields were given.

conditions for product **3aa** (Fig. 5a). As expected, 2,5-dihydropyrrole **3aa** was obtained successfully in 62% yield, demonstrating that allene **5aa** likely serves as a reactive intermediate. Next, deuterium labeling using CD₃OD as the source afforded **3aa-d**, revealing significant deuterium incorporation at both the 2- and 3-positions of the pyrrole ring (Fig. 5b). This H/D scrambling indicates that reversible protonation/deprotonation steps occur at these sites. Kinetic studies of the sequential hydroamination revealed a pronounced ligand effect. The reaction proceeded significantly faster using 5.0 mol% Pd(acac)₂ and

2.5 mol% XantPhos (excess Pd) than with a 1:1 molar ratio (XantPhos/Pd(acac)₂) (Fig. 5c). Subsequent kinetic experiments using isolated allene **5aa** demonstrated that added ligand slowed down the annulation step (Fig. 5d). Replacing Pd(acac)₂ with Pd(dba)₂ significantly inhibited the annulation. This observation, combined with the ligand effects, suggests Pd(II) species may function as Lewis acid catalysts in the intramolecular hydroamination step^{60–62}. Supporting this hypothesis, control experiments showed Cu(OAc)₂ also catalyzes this transformation (Supplementary Table 13 for details).

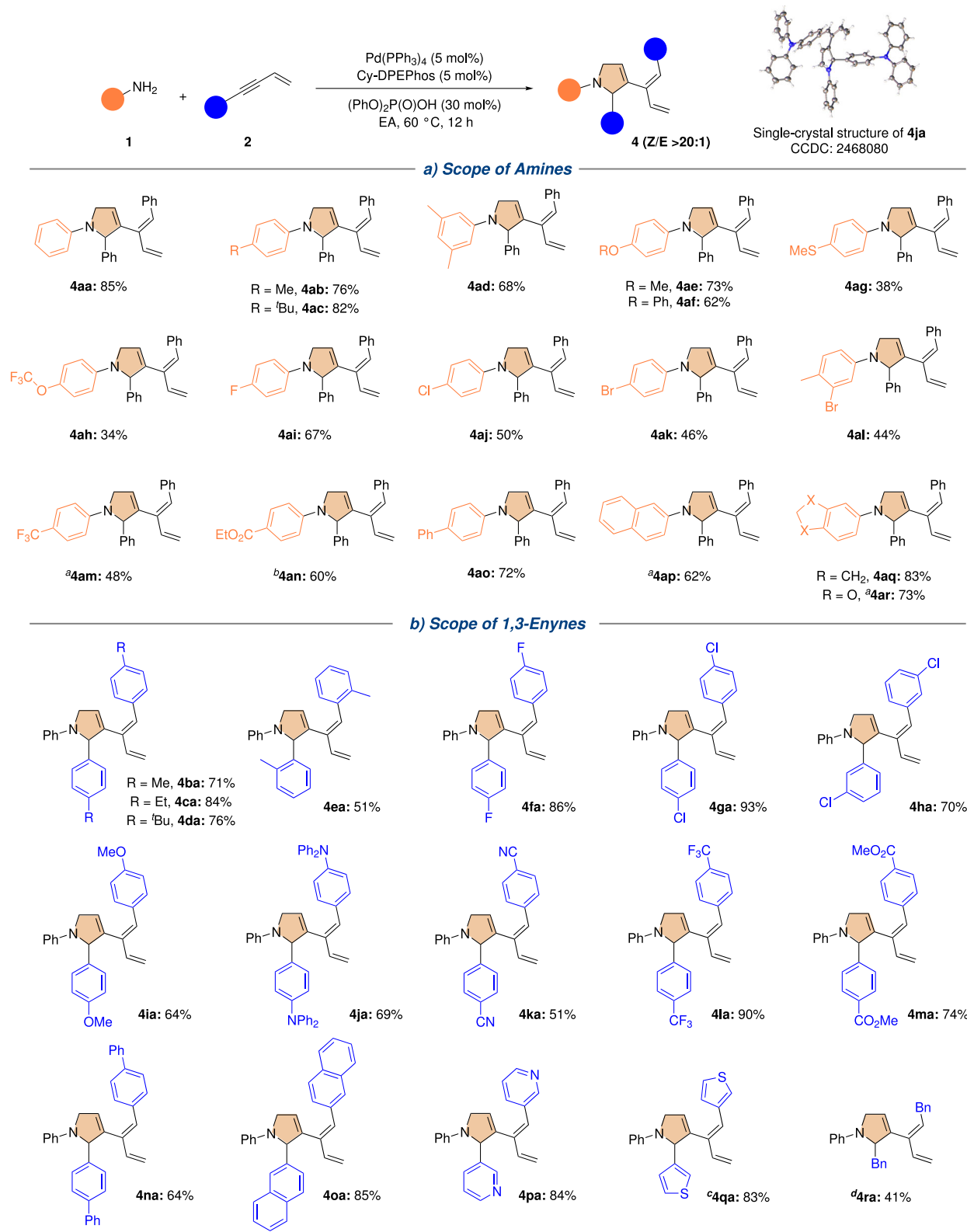


Fig. 4 | Substrate scope for Pd-catalyzed telomerization of 1,3-enynes with amines. a Scope of Amines. **b** Scope of 1,3-Enynes. Condition: **1** (0.10 mmol), **2** (3.0 eq.), Pd(PPh₃)₄ (5 mol%), Cy-DPEPhos (5 mol%), (PhO)₂P(O)OH (30 mol%), EA

(0.5 mL), 60 °C, 12 h. Isolated yields were given. Unless otherwise noted, all the ratio of Z/E of substrates were >20:1. ^a70 °C. ^b80 °C. ^cZ/E = 18:1. ^dZ/E = 4:1.

Further experiments were also conducted to probe the mechanistic details of the telomerization process (Fig. 5e–h). Direct coupling between **3aa** and 1,3-enyne **2a** failed to produce telomeric product **4aa** (Fig. 5e), eliminating **3aa** as an intermediate in this pathway. Reacting

isolated allene **5aa** with an additional equivalent of **2a** successfully afforded **4aa** in 48% yield (Fig. 5f, entry 1), identifying **5aa** as the key intermediate for the telomerization pathway. However, this transformation was completely suppressed when using Pd(acac)₂ instead of

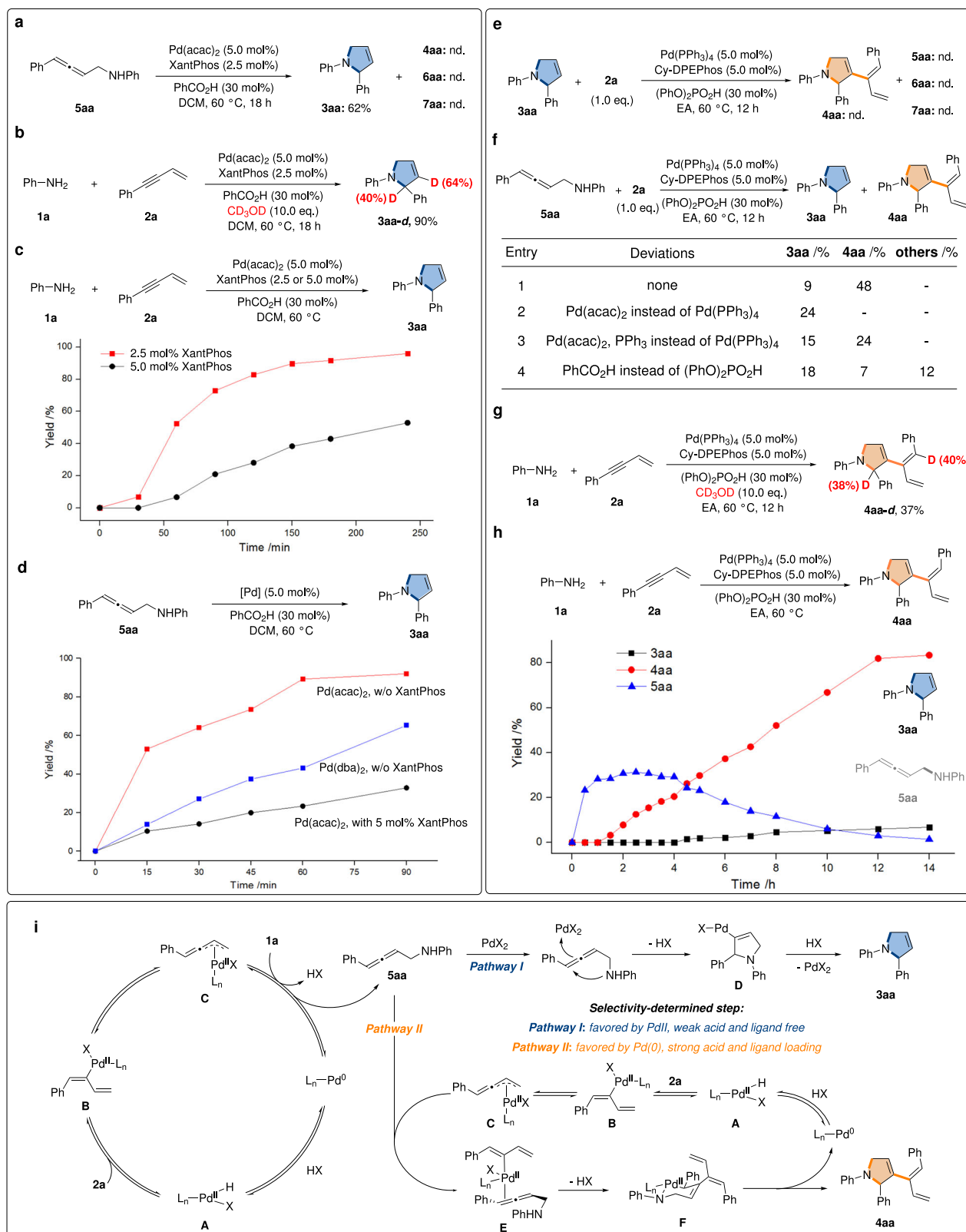


Fig. 5 | Mechanistic experiments and proposed mechanism. a Interconversion of intermediate for **3aa**. **b** Deuterium-labeling study of **3aa**. **c** Kinetic studies for **3aa**. **d** Kinetic studies for intermediate **5aa**. **e** Interconversion of **3aa** to **4aa**. **f** Control

experiments for **4aa**. **g** Deuterium-labeling study of **4aa**. **h** Kinetic studies for **4aa** under standard conditions. **i** Proposed mechanism.

$\text{Pd}(\text{PPh}_3)_4$ (Fig. 5f, entry 2). This aligns with observations in Fig. 5d, confirming that $\text{Pd}(\text{II})$ precursors accelerate the intramolecular hydroamination of **5aa** to **3aa**, thereby diverting selectivity away from telomerization. Supplementing additional ligand effectively impeded

the annulation of **5aa**, promoting **4aa** formation (Fig. 5f, entry 3). In addition, replacing $(\text{PhO})_2\text{PO}_2\text{H}$ with the weaker acid PhCO_2H favored formation of **3aa** (Fig. 5f, entry 4), consistent with the selectivity control shown in Fig. 2a. Deuterium labeling (CD_3OD) in the telomerization

of **1a** and **2a** revealed significant H/D exchange at the pyrroline 2-position and the 1-position of the 1,3-butadienyl group in **4aa-d** (Fig. 5g). This suggests the pathway involves alkene insertion between the pyrroline moiety and an alkenyl-Pd species (generated via 1,2-insertion of a Pd-hydride into **2a**), followed by intramolecular C–N coupling. Besides, kinetic monitoring of the telomerization reaction detected intermediate **5aa** in the early stages, with its gradual consumption coinciding with **4aa** formation (Fig. 5h), supporting the proposed sequence. Crossover experiments using **5aa** as the starting material for both the annulation and telomerization pathways yielded cross-annulated products (Supplementary Figs. 5 and 6). These results demonstrate the reversibility associated with the formation of allene intermediate **5aa**.

Based on the above results and previous literature^{60,63,64}, a plausible mechanism for this chemodivergent coupling reaction was proposed (Fig. 5i). First, an oxidative addition between Pd(O) species and acid HX yields Pd(II)-H intermediate **A**. Then, 1,3-enyne **2a** undergoes regioselective migratory insertion into Pd(II)-H species to afford alkenyl-palladium **B**, which can be reversibly converted to π -allyl palladium species **C**. Next, aniline **1a** undergoes nucleophilic attack on π -allyl palladium intermediate, releasing one molecule of HX and allene intermediate **5aa**, as well as the regeneration of Pd(O) species. Under condition A, which is performed with weak acid PhCO₂H and half equivalent of bidentate ligand (XantPhos/Pd= 1:2), the allene **5aa** is directly activated by Pd(II), followed by nucleophilic attack on the 2-positions of allene, furnishing a vinyl palladium species **D**. Finally, species **D** undergoes protonolysis to give annulated product **3aa** and recycle Pd(II) catalyst (Pathway I). Under condition B, however, the addition of strong acid (PhO)₂PO₂H may facilitate the formation of Pd(II)-hydride species and thus accelerate the alkyne insertion to deliver intermediate **B** and its tautomer **C**. Meanwhile, the excessive dosages of ligand (XantPhos/Pd= 1:1) can impede the direct intramolecular amination of allene **5aa**. As a result, complex **E** may be preferentially formed through the coordination between allene **5aa** and intermediate **C** (Pathway II). After an allene insertion, cyclopalladated intermediate **F** is generated which then proceeds through a final reductive elimination to furnish telomerization product **4aa** and regenerates palladium catalyst. Notably, the reaction of allene **5aa** proceeds much faster via Pathway I (intramolecular hydroamination) than Pathway II (telomerization) in the presence of Pd(II) catalysts. Consequently, modulating the relative rate of this step directly governs product selectivity. By replacing Pd(II) with Pd(O) precursors, employing strong acids, and using excess ligand, the reaction pathway can be efficiently diverted toward the telomeric product **4aa**.

Synthetic transformations

Encouraged by the generality of this chemodivergent strategy, we carried out the late-stage modification of a series of bioactive molecules featuring the aniline motif (Fig. 6a). Procaine and dimethocaine, two widely applied and effective anesthetics, could react with 1,3-enyne **2a** and generate 2,5-dihydropyrroles **8** and **9** in medium to good yields. For molecules bearing amide N-H groups, like sulfalen, this protocol also enabled successful modification in 36% yield (**10**). Coumarin 120, an arylamine with fused-ring framework, could also deliver the target product **11** in 56% yield smoothly at a higher reaction temperature. The acetanilide derivatives could still undergo this process to afford the corresponding products **13** and **14** with good yields and excellent Z/E selectivities. Other modification products could be concisely prepared in decent yields and satisfactory Z/E selectivities from arylamine molecular drugs with different scaffolds (**15–17**). Due to the poor solubility, the telomerization of coumarin 120 with two molecules of **2a** exhibited a decline in yield (**16**).

To demonstrate the practicality of this protocol, scale-up reactions and various transformations were performed (Figs. 6b, 5c). The protocol could proceed unimpededly in 2 mmol scale, affording **3aa** in

88% yield. The oxidative aromatization or reductive hydrogenation of **3aa** was conducted successfully, resulting in the formation of corresponding products **18** or **19** in excellent yield. Recently, the skeleton editing of *N*-heterocyclic frameworks has become an appealing tool for the assembly of molecular complexity. Inspired by the ring-expansion of saturated amines recently developed by Wang and co-workers⁶⁵, we wondered whether hemi-saturated product **3aa** could also undergo such alkyne insertion reactions. To our surprise, submitting **3aa** and alkynyl ester to the reaction system, cycloaddition occurred following by ring-opening rather than alkyne insertion, providing an unexpected product **20** in 34% isolated yield. The structure was confirmed by single-crystal X-ray crystallography after hydrolysis (**21**, CCDC: 2472318). Additionally, scale-up reaction for **4aa** was achieved in 87% yield with excellent Z/E selectivity (Fig. 6c). To our delight, the stereoselective oxidative aromatization of telomerization product **4aa** could be conducted successfully. In the presence of MnO₂, aromatization product **22** in *Z*-configuration could be obtained in excellent selectivity. In comparison, the stereoselectivity could be efficiently switched to *E*-configuration under the irradiation of white LED in air. The structure of compound **22** (*E*) was unambiguously confirmed by single-crystal X-ray crystallographic analysis (CCDC: 2468081). Besides aromatization, product **4aa** could occur 1,4-hydroborylation/oxidation to provide allylic alcohol **23** in 59% yield with exclusive *E*-stereoselectivity under Ni catalysis. In addition, a Co-catalyzed Simmons–Smith-type cyclopropanation was also applicable and afforded highly substituted dihydropyrroles **24** with high *Z*-selectivity. Thienyl-substituted polysubstituted pyrrole **25**, which are difficult to obtain via conventional synthetic methods, could also be accessed by oxidative cyclization reactions between inorganic sulfurating reagent K₂S and **4aa**. Finally, hydrogenation furnished alkyl-substituted dihydropyrrole **26** in 61% yield.

In conclusion, we have developed a chemodivergent Pd-catalyzed protocol for the construction of multi-substituted 2,5-dihydropyrrole scaffolds. Employing weak acid additives and a Pd(II) precursor enables the rapid sequential hydroamination of 1,3-enynes with amines, affording 2-substituted 2,5-dihydropyrroles. Conversely, switching to strong acids and Pd(O) precursors efficiently redirects chemoselectivity towards the telomerization pathway, delivering 3-(buta-1,3-dienyl)-substituted 2,5-dihydropyrroles with excellent Z/E selectivities. Mechanistic studies elucidated that ligand loading significantly influences reaction outcomes by modulating the annulation rate of the allenylamine intermediate. This strategy features broad functional group tolerance, facilitates late-stage modification of bioactive molecules, and enables diverse derivatizations. Compared to conventional methods, this protocol provides an unprecedented and direct route to functionalized 2,5-dihydropyrrole scaffolds from readily available starting materials in an atom-economical fashion.

Methods

General procedure for palladium-catalyzed sequential hydroamination of 1,3-enynes with amines

In a nitrogen glove box, Pd(acac)₂ (0.01 mmol, 3.0 mg), XantPhos (0.005 mmol, 2.9 mg) and PhCO₂H (0.06 mmol, 7.2 mg) were added in an oven-dried 4 mL vial. Then, freshly distilled DCM (1.0 mL) and 1,3-enyne **2** (0.4 mmol) were injected to the sealed vial. Finally, amine **1** (0.2 mmol) was added. The reaction vial was sealed with a cap, removed from the glove box. The reaction mixture was stirred at 60 °C for 18 hours. The crude reaction mixture was purified by column chromatography on silica gel using petroleum ether and ethyl acetate to afford the corresponding product **3**.

General procedure for palladium catalyzed telomerization of 1,3-enynes with amines

In a nitrogen glove box, Pd(PPh₃)₄ (0.005 mmol, 5.8 mg), Cy-DPEPhos (0.005 mmol, 2.8 mg) and (PhO)₂P(O)OH (0.03 mmol, 7.5 mg) were

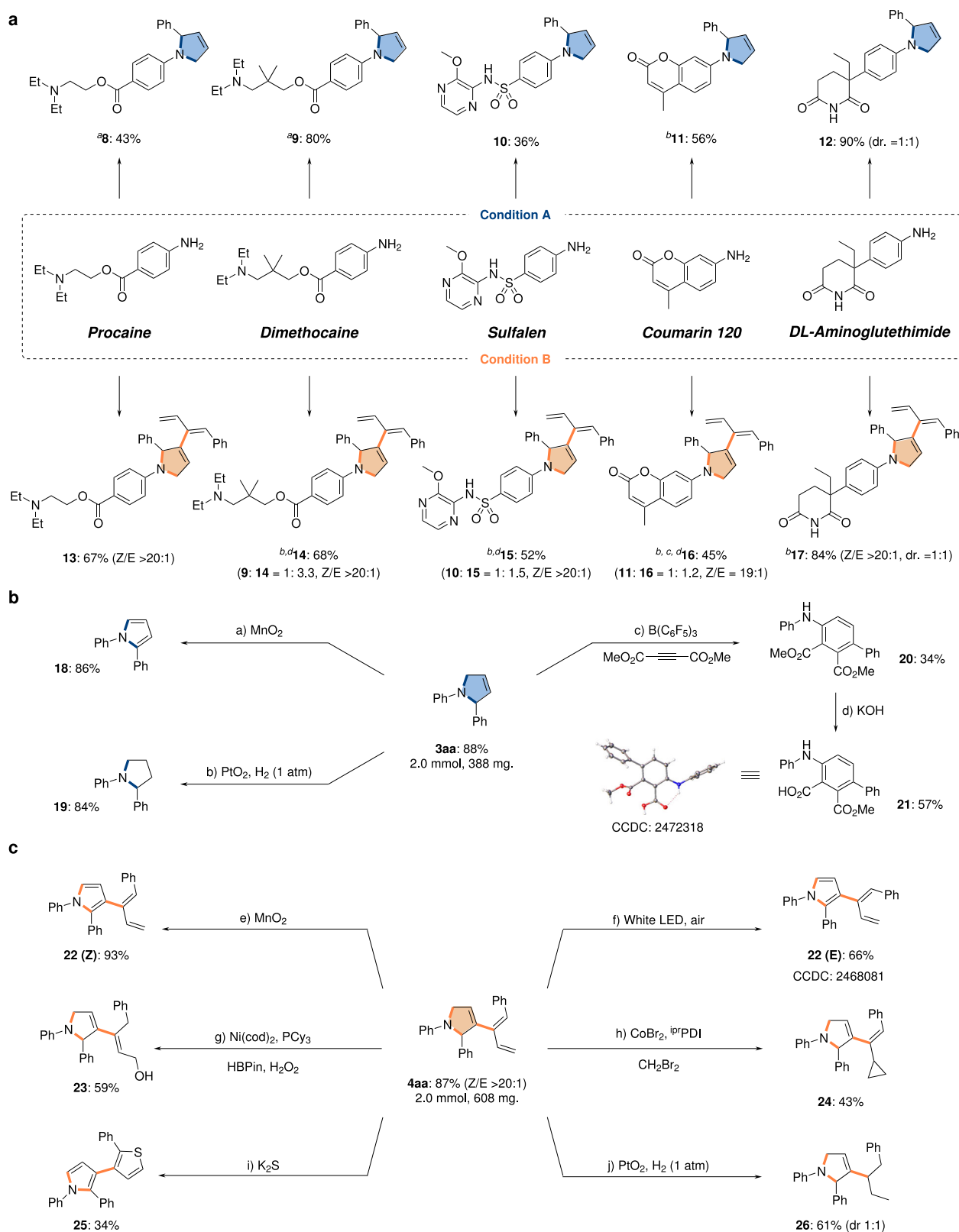


Fig. 6 | Synthetic utilization. **a** Late-stage modifications. Condition A: aniline (0.10 mmol), **2a** (2.0 eq.), Pd(acac)₂ (5 mol%), XantPhos (2.5 mol%), PhCO₂H (30 mol%), DCM (0.5 mL), 60 °C, 18 h. Condition B: aniline (0.10 mmol), **2a** (3.0 eq.),

Pd(PPh₃)₄ (5 mol%), Cy-DPEPhos (5 mol%), (PhO)₂P(O)OH (30 mol%), EA (0.5 mL), 60 °C, 12 h. ^aPhCO₂H (1.0 eq.). ^b80 °C. ^cEA (1.0 mL). ^d¹H-NMR yield. **b** Scale-up reaction and derivatizations of **3aa**. **c** Scale-up reaction and derivatizations of **4aa**.

added in an oven-dried 4 mL vial. Then, freshly distilled EA (0.5 mL) and 1,3-enyne **2** (0.3 mmol) were injected into the sealed vial. Finally, amine **1** (0.1 mmol) was added. The reaction vial was sealed with a cap, removed from the glove box. The reaction mixture was stirred at 60 °C

for 12 hours. The crude reaction mixture was purified by column chromatography on silica gel using petroleum ether and ethyl acetate to afford the corresponding product **4**. The Z/E ratios of products were determined by ¹H NMR analysis.

Data availability

The X-ray crystallographic data for compounds have been deposited in the Cambridge Crystallographic Data Centre (CCDC) under deposition numbers CCDC 2468082 (**3aa**), 2468080 (**4ja**), 2472318 (**21**), 2468081 (**22 E**) and 2519020 (**S-3aa**). Data relating to the characterization data of materials and products, general methods, optimization studies, experimental procedures, mechanistic studies, mass spectrometry and NMR spectra are available in the Supplementary Information. All data are also available from the corresponding author upon request.

References

1. Beletskaya, I. P., Nájera, C. & Yus, M. Stereodivergent catalysis. *Chem. Rev.* **118**, 5080–5200 (2018).
2. Li, L., Chen, Z., Zhang, X.-W. & Jia, Y.-X. Divergent strategy in natural product total synthesis. *Chem. Rev.* **118**, 3752–3832 (2018).
3. Nájera, C., Beletskaya, I. P. & Yus, M. Metal-catalyzed regiodivergent organic reactions. *Chem. Soc. Rev.* **48**, 4515–4618 (2019).
4. Beletskaya, I. P., Nájera, C. & Yus, M. Chemodivergent reactions. *Chem. Soc. Rev.* **49**, 7101–7166 (2020).
5. Chintawar, C. C., Yadav, A. K., Kumar, A., Sancheti, S. P. & Patil, N. T. Divergent gold catalysis: Unlocking molecular diversity through catalyst control. *Chem. Rev.* **121**, 8478–8558 (2021).
6. Viji, M. et al. Regiodivergent organocatalytic reactions. *Catalysts* **11**, 1013–1058 (2021).
7. Sakakibara, Y. & Murakami, K. Switchable divergent synthesis using photocatalysis. *ACS Catal.* **12**, 1857–1878 (2022).
8. Chaudhary, H. R. & Patel, D. M. Recent trends for chemoselectivity modulation in one-pot organic transformations. *RSC Adv.* **14**, 31072–31116 (2024).
9. Chakraborty, G. & Maity, S. Divergent hydroelementation of unsaturated C–C bonds using 3d transition metal based catalysts. *Adv. Synth. Catal.* **367**, e202401239 (2025).
10. Bhutani, P. et al. U.S. FDA approved drugs from 2015–june 2020: A perspective. *J. Med. Chem.* **64**, 2339–2381 (2021).
11. Marshall, C. M., Federice, J. G., Bell, C. N., Cox, P. B. & Njardarson, J. T. An update on the nitrogen heterocycle compositions and properties of U.S. FDA-approved pharmaceuticals (2013–2023). *J. Med. Chem.* **67**, 11622–11655 (2024).
12. Vitaku, E., Smith, D. T. & Njardarson, J. T. Analysis of the structural diversity, substitution patterns, and frequency of nitrogen heterocycles among U.S. FDA approved pharmaceuticals. *J. Med. Chem.* **57**, 10257–10274 (2014).
13. Pennington, L. D. & Moustakas, D. T. The necessary nitrogen atom: A versatile high-impact design element for multiparameter optimization. *J. Med. Chem.* **60**, 3552–3579 (2017).
14. Kerru, N., Gummidu, L., Maddila, S., Gangu, K. K. & Jonnalagadda, S. B. A review on recent advances in nitrogen-containing molecules and their biological applications. *Molecules* **25**, 1909–1951 (2020).
15. Anderson, W. K. & Milowsky, A. S. 3-Pyrroline N-oxide bis(carbamate) tumor inhibitors as analogues of indicine N-oxide. *J. Med. Chem.* **30**, 2144–2147 (1987).
16. Fraley, M. E. et al. Kinesin spindle protein (KSP) inhibitors. Part 2: The design, synthesis, and characterization of 2,4-diaryl-2,5-dihydropyrrole inhibitors of the mitotic kinesin KSP. *Bioorg. Med. Chem. Lett.* **16**, 1775–1779 (2006).
17. Shi, W. et al. Design, synthesis, and antibacterial activity of 2,5-dihydropyrrole formyl hydroxyamino derivatives as novel peptide deformylase inhibitors. *Bioorg. Med. Chem. Lett.* **20**, 3592–3595 (2010).
18. Medran, N. S., La-Venia, A. & Testero, S. A. Metal-mediated synthesis of pyrrolines. *RSC Adv.* **9**, 6804–6844 (2019).
19. Fu, G. C., Nguyen, S. T. & Grubbs, R. H. Catalytic ring-closing metathesis of functionalized dienes by a ruthenium carbene complex. *J. Am. Chem. Soc.* **115**, 9856–9857 (1993).
20. Moonen, K., Dieltiens, N. & Stevens, C. V. Synthesis of 2-phosphonopyrroles via a one-pot RCM/oxidation sequence. *J. Org. Chem.* **71**, 4006–4009 (2006).
21. Bunrit, A., Sawadjoon, S., Tšupova, S., Sjöberg, P. J. R. & Samec, J. S. M. A general route to β -substituted pyrroles by transition-metal catalysis. *J. Org. Chem.* **81**, 1450–1460 (2016).
22. Groso, E. J. et al. 3-Aryl-2,5-Dihydropyrroles via catalytic carbonyl-olefin metathesis. *ACS Catal.* **8**, 2006–2011 (2018).
23. Zhang, D. H., Yao, L. F., Wei, Y. & Shi, M. Gold(I)-catalyzed cycloisomerization of 1,6-diyne: synthesis of 2,3-disubstituted 3-pyrroline derivatives. *Angew. Chem. Int. Ed.* **50**, 2583–2587 (2011).
24. Zhang, D.-H., Zhang, Z. & Shi, M. Transition metal-catalyzed carbocyclization of nitrogen and oxygen-tethered 1,n-enynes and diynes: Synthesis of five or six-membered heterocyclic compounds. *Chem. Commun.* **48**, 10271–10279 (2012).
25. Yang, J.-M. et al. Rhodium(III)-catalyzed intramolecular cyclization and sequential aromatization of ynamides with propargyl esters: Access to 2,5-dihydropyrroles and pyrroles. *Org. Lett.* **26**, 6191–6196 (2024).
26. Morit, N. & Krause, N. Gold catalysis in organic synthesis: Efficient cycloisomerization of α -aminoallenes to 3-pyrrolines. *Org. Lett.* **6**, 4121–4123 (2004).
27. Sai, M., Yorimitsu, H. & Oshima, K. Allyl-, allenyl-, and propargyl-transfer reactions through cleavage of C–C bonds catalyzed by an n-heterocyclic carbene/copper complex: Synthesis of multi-substituted pyrroles. *Angew. Chem. Int. Ed.* **50**, 3294–3298 (2011).
28. Brioché, J., Meyer, C. & Cossy, J. Synthesis of functionalized allenamides from ynamides by enolate Claisen rearrangement. *Org. Lett.* **15**, 1626–1629 (2013).
29. Rajasekaran, T., Karthik, G., Sridhar, B. & Reddy, B. V. S. Dual behavior of isatin-based cyclic ketimines with dicarbomethoxy carbene: Expedient synthesis of highly functionalized spirooxindolyl oxazolidines and pyrrolines. *Org. Lett.* **15**, 1512–1515 (2013).
30. Xie, H.-D. et al. A copper-catalyzed annulation reaction of diazo esters with propargyl amines for the synthesis of 2,5-dihydropyrroles. *Org. Chem. Front.* **11**, 4546–4555 (2024).
31. Zhang, Z. et al. Enantioselective propargylic amination and related tandem sequences to α -tertiary ethynylamines and azacycles. *Nat. Chem.* **16**, 521–532 (2024).
32. Radhakrishnan, U., Al-Masum, M. & Yamamoto, Y. Palladium catalyzed hydroamination of conjugated enynes. *Tetrahedron Letters* **39**, 1037–1040 (1998).
33. Zhang, W., Werness, J. B. & Tang, W. Intramolecular hydroamination of conjugated enynes. *Tetrahedron* **65**, 3090–3095 (2009).
34. Zhang, Y., Yu, B., Gao, B., Zhang, T. & Huang, H. Triple-bond insertion triggers highly regioselective 1,4-aminomethylamination of 1,3-enynes with aminals enabled by Pd-catalyzed C–N bond activation. *Org. Lett.* **21**, 535–539 (2019).
35. Li, L. et al. Direct access to spirocycles by Pd/wingphos-catalyzed enantioselective cycloaddition of 1,3-enynes. *Nat. Commun.* **12**, 5667–5677 (2021).
36. Cera, G. & Maestri, G. Palladium/Brønsted acid catalysis for hydrofunctionalizations of alkynes: From Tsuji–Trost allylations to stereoselective methodologies. *ChemCatChem* **14**, e202200295 (2022).
37. Li, Q.-Y., Fang, X.-X., Pan, R., Yao, H.-Q. & Lin, A.-J. Palladium-catalyzed asymmetric sequential hydroamination of 1,3-enynes: Enantioselective syntheses of chiral imidazolidinones. *J. Am. Chem. Soc.* **144**, 11364–11376 (2022).
38. Lu, W.-X., Zhao, Y.-M. & Meng, F.-K. Cobalt-catalyzed sequential site- and stereoselective hydrosilylation of 1,3- and 1,4-enynes. *J. Am. Chem. Soc.* **144**, 5233–5240 (2022).
39. Li, L., Wang, S., Jakhar, A. & Shao, Z.-H. Pd-catalyzed functionalization of 1,3-enynes via alkylene- π -allylpalladium intermediates. *Green Synth. Catal.* **4**, 124–134 (2023).

40. Li, R., Zhang, H., Yu, B. & Huang, H. Chemo- and regioselective cyclization of diene-tethered enynes via palladium-catalyzed aminomethylation. *Org. Chem. Front.* **10**, 2988–2993 (2023).
41. Wang, H., Jie, X.-F., Chong, Q.-L. & Meng, F.-K. Pathway-divergent coupling of 1,3-enynes with acrylates through cascade cobalt catalysis. *Nat. Commun.* **15**, 3427–3436 (2024).
42. Wang, S. et al. Stereodivergent synthesis of chiral spiropyrazolones through Pd-catalyzed asymmetric sequential hydroalkylation of 1,3-enynes: unusual solvent effects on the enantioselectivity. *Org. Chem. Front.* **11**, 3033–3040 (2024).
43. Xie, B.-Y. & He, Z.-T. Chemodivergent tandem hydroalkylation and hydroalkenoxylation of conjugated enynes. *ACS Catal.* **14**, 9742–9751 (2024).
44. Hu, Y. et al. Nickel-catalyzed asymmetric three-component reaction of unactivated alkyl halides, 1,3-enynes and aldehydes. *Angew. Chem. Int. Ed.* **65**, e20212 (2026).
45. Jin, P.-S., He, X.-Q., Liu, S.-S., Qi, X.-T. & Shen, X. Synthesis of tri-fluoromethylated 2H-pyrans enabled by Pd-catalyzed cascade cyclization of trifluoroacetylsilanes and 1,3-enynes. *CCS Chem.* **8**, 1267–1275 (2026).
46. Pagar, V. V. & RajanBabu, T. V. Tandem catalysis for asymmetric coupling of ethylene and enynes to functionalized cyclobutanes. *Science* **361**, 68–72 (2018).
47. Zatochnaya, O. V. & Gevorgyan, V. Synthesis of fluoro- and perfluoroalkyl arenes via palladium-catalyzed [4 + 2] benzannulation reaction. *Org. Lett.* **15**, 2562–2565 (2013).
48. Zhang, Z. & Gevorgyan, V. Escape from hydrofunctionalization: Palladium hydride-enabled difunctionalization of conjugated dienes and enynes. *Angew. Chem. Int. Ed.* **62**, e202311848 (2023).
49. Yang, Z.-R. et al. Onestone three birds: Ni-catalyzed asymmetric allenic substitution of allenic ethers, hydroalkylation of 1,3-enynes and double alkylation of enynyl ethers. *Chin. Chem. Lett.* **35**, 109518–109523 (2024).
50. Hu, Y. C., Ji, D. W., Zhao, C. Y., Zheng, H. & Chen, Q. A. Catalytic prenylation and reverse prenylation of indoles with isoprene: Regioselectivity manipulation through choice of metal hydride. *Angew. Chem. Int. Ed.* **58**, 5438–5442 (2019).
51. Jiang, W. S. et al. Orthogonal regulation of nucleophilic and electrophilic sites in Pd-catalyzed regiodivergent couplings between indazoles and isoprene. *Angew. Chem. Int. Ed.* **60**, 8321–8328 (2021).
52. Zhao, C. Y. et al. Bioinspired and ligand-regulated unnatural prenylation and geranylation of oxindoles with isoprene under Pd. *Catalysis. Angew. Chem. Int. Ed.* **61**, e202207202 (2022).
53. Yang, S.-N. et al. Ni-catalyzed regiodivergent hydrophosphorylation of enynes. *Chin. Chem. Lett.* **34**, 107914 (2023).
54. Zhang, W.-N. et al. Ligand-controlled regiodivergence in Pd-catalyzed coupling of azlactones with isoprene. *Cell Rep. Phys. Sci.* **5**, 101908 (2024).
55. Adamson, N. J., Jeddi, H. & Malcolmson, S. J. Preparation of chiral allenes through Pd-catalyzed intermolecular hydroamination of conjugated enynes: enantioselective synthesis enabled by catalyst design. *J. Am. Chem. Soc.* **141**, 8574–8583 (2019).
56. Sakai, N., Ridder, A. & Hartwig, J. F. Tropene derivatives by sequential intermolecular and transannular, intramolecular palladium-catalyzed hydroamination of cycloheptatriene. *J. Am. Chem. Soc.* **128**, 8134–8135 (2006).
57. Yang, X.-H., Lu, A. & Dong, V. M. Intermolecular hydroamination of 1,3-dienes to generate homoallylic amines. *J. Am. Chem. Soc.* **139**, 14049–14052 (2017).
58. Tang, M.-Q., Yang, Z.-J. & He, Z.-T. Asymmetric formal sp²-hydrocarbonations of dienes and alkynes via palladium hydride catalysis. *Nat. Commun.* **14**, 6303 (2023).
59. Kuai, C.-S., Wang, Y.-R., Yang, T. & Wu, X.-F. Multimodal precise control over multiselective carbonylation of 1,3-enynes. *J. Am. Chem. Soc.* **147**, 7950–7964 (2025).
60. Asao, N., Nogami, T., Takahashi, K. & Yamamoto, Y. Pd(II) Acts simultaneously as a Lewis acid and as a transition-metal catalyst: Synthesis of cyclic alkenyl ethers from acetylenic aldehydes. *J. Am. Chem. Soc.* **124**, 764–765 (2002).
61. Xiao, Y.-J. & Zhang, J.-L. Tetrasubstituted furans by a Pd^{II}-catalyzed three-component Michael addition/cyclization/cross-coupling reaction. *Angew. Chem. Int. Ed.* **47**, 1903–1906 (2008).
62. Zhang, J.-B. & Han, X.-L. An unexpected addition of acetic acid to ortho-electron-deficient alkynyl-substituted aryl aldehydes catalyzed by palladium(II) acetate. *Adv. Synth. Catal.* **356**, 2465–2470 (2014).
63. Li, L., Luo, P.-F., Deng, Y.-H. & Shao, Z.-H. Regioselectivity switch in palladium-catalyzed allenic cycloadditions of allenic esters: [4+1] or [4+3] Cycloaddition/cross-coupling. *Angew. Chem. Int. Ed.* **58**, 4710–4713 (2019).
64. Luo, P.-F. et al. Switchable chemo-, regio- and pseudo-stereodivergence in palladium-catalyzed cycloaddition of allenes. *Angew. Chem. Int. Ed.* **63**, e202412179 (2024).
65. Zhou, X.-Y., Liu, L., Lyu, H. & Wang, X.-C. Modular alkyl growth in amines via the selective insertion of alkynes into C–C bonds. *Nat. Chem.* **17**, 1323–1330 (2025).

Acknowledgements

Financial support from the National Natural Science Foundation of China (22201281) and the Natural Science Foundation of Liaoning Province (2025-MS-055) is acknowledged.

Author contributions

Q.-A. C. conceived and supervised the project. Q.-A. C., S.-Y. X. and D.-W. J. designed the experiments. S.-Y. X., D.-W. J., X.-T. L. and Z.-H. W. performed the experiments and analyzed the data. All authors discussed the results and commented on the manuscript.

Competing interests

The authors declare no competing interests.

Additional information

Supplementary information The online version contains supplementary material available at <https://doi.org/10.1038/s41467-026-70201-z>.

Correspondence and requests for materials should be addressed to Ding-Wei Ji or Qing-An Chen.

Peer review information *Nature Communications* thanks Zhihui Shao, and the other, anonymous, reviewer for their contribution to the peer review of this work. A peer review file is available.

Reprints and permissions information is available at <http://www.nature.com/reprints>

Publisher's note Springer Nature remains neutral with regard to jurisdictional claims in published maps and institutional affiliations.

Open Access This article is licensed under a Creative Commons Attribution-NonCommercial-NoDerivatives 4.0 International License, which permits any non-commercial use, sharing, distribution and reproduction in any medium or format, as long as you give appropriate credit to the original author(s) and the source, provide a link to the Creative Commons licence, and indicate if you modified the licensed material. You do not have permission under this licence to share adapted material derived from this article or parts of it. The images or other third party material in this article are included in the article's Creative Commons licence, unless indicated otherwise in a credit line to the material. If material is not included in the article's Creative Commons licence and your intended use is not permitted by statutory regulation or exceeds the permitted use, you will need to obtain permission directly from the copyright holder. To view a copy of this licence, visit <http://creativecommons.org/licenses/by-nc-nd/4.0/>.

© The Author(s) 2026